Design and Testing Outline for a Free Running Model of a High Speed Craft

Xinguo WANG [a,b], Jack BONOLI [a], Madeline COHEN [a] and Mirjam FÜRTH [c,1]
[a] *Stevens Institute of Technology, Hoboken, NJ*
[b] *KTH Royal Institute of Technology, Stockholm, Sweden*
[c] *Texas A&M University, College Station, TX*

Abstract. Hydrodynamics of High Speed Craft is a topic of very high interest for recreational boaters and industry professionals alike. This project aims to be a first step toward conducting such experiments in exposed outdoor environments. This paper will outline a preliminary design and testing plan of a free running model of a high speed craft. The proposed free running model will be subjected to all six degrees of freedom, self propelled, autonomously controlled, and will be exposed to weather elements.

Keywords. High Speed Craft, Free Running Model, Model Parameter Analysis, PD Controller, Environment Monitoring

1. Introduction

To better understand the flow phenomena associated with HSC, more experiments are needed. The vast majority of experimental studies on HSC have taken place in high speed towing tanks [1] [2] [3] [4]. Free running tests have been recommended to evaluate surge motion of HSC [5]. However, the use of free running models in open settings is much less common, especially for HSC. Unlike towing tank tests, free running tests are exposed to various environmental factors and require propulsion, steering, and sensor systems on-board the model. Free running tests will expose the model to all six degrees of freedom and environmental factors. The unpredictability and non-uniformity of wind, waves, and currents makes some aspects of testing with a free running model more difficult, as wind, wave and current conditions can introduce error. However, if and only if closely monitored, tests in these conditions can provide valuable insights [6].

Few free running model tests of HSC craft have been conducted. In Larson's thesis [7], a specific scale was not used to guide free running model design and construction, rather a model length of 1.2 m was chosen so that standard hobby components for model racing boats could be used onboard. Carbon Fiber reinforced composite was used to keep the model at a convenient weight while remaining sufficiently durable. Kim and Kim [8] designed a high speed free running model of 1:2.3 scale (length 3.4 m and weight 231.8 kg) to perform turning tests. To calculate the resistance, an estimation was used based

[1] Corresponding Author: Mirjam Fürth, Department of Ocean Engineering, Texas A&M University, College Station, Texas, 77840, Email: furth@tamu.edu

on the resistance of a 1:65 model that was tested with a tow-carriage. The differences in turning characteristics between high speed planing craft and displacement ships such as the slip phenomena were evaluated. Whereas, large-scale free running tests at 1:19 scale (model length 7.06 m), based on a Chinese navy ship of about 134 m with a hybrid monohull, were carried out by [6]. They compared the seakeeping of the free running model to smaller scale towing tank tests of 1:40 scale and 2.5D theoretical calculations. Despite the disadvantages of the uncontrolled environment, the large-scale free running tests still showed potential as a supplement to towing tank testing. High speed, free running, radio controlled tests of a self propelled 1:9 scale model (length 1.524m) of a 47 ft life boat were conducted in Davidson Laboratory in 1993 [9]. The testing aimed to study the roll characteristics of the model when in turn. Testing successfully demonstrated the same "snap roll" phenomenon that had been observed in the full scale lifeboat, which bodes well for the validity of free running tests. Furthermore, Free running model test on the Duisburg Rowing course of high speed craft were carried out by Friedhoff and Feller [10] to complement tank testing using a 1:6 scale model (model length 2.67 m). They concluded that, indoor towing tank tests showed more accurate measurements, while free free running tests demonstrated running characteristics such as maneuvering and accelerating.

The aim of this paper is to present a design concept for a free running model for testing *in situ*. The design comprises of a Computer Aided Design (CAD) modeled hull is proposed based on a detailed parameter analysis, a propulsion system that will achieve the required amount of thrust based on the speed to length ratios of existing HSC is detailed and a steering system that utilizes Inertial Measurement Units (IMU's) and a proportional-derivative (PD) controller. Furthermore, sensor implementation to record necessary performance data is explored and the requirements for eventual testing locations where the model will be used are detailed.

2. Model Design and Specifications

2.1. Hull Parameter Analysis

The free running model will be constructed so that the hull can be altered, and allow the drive train and sensors to be moved and retrofitted.

The hull presented in this paper is designed for investigations of the effect of detaching the flow in the spray area, by the use of spray detaching technologies such as spray rails [3] [4] [11] and spray deflectors [2] [12] [13]. Whisker spray develops along the hull as the craft moves through the water, and can account for 15% to 20% of total high speed craft resistance [14] [15]. Previous investigations have shown that when the spray resistance component is low, changes due to reflection of spray have been hard to measure [13]. Therefore, the design priority is to maximize the spray resistance, so that the resistance reduction becomes clearly measurable in absolute numbers. Particulars which have direct influence on spray resistance are beam, deadrise angle and model weight [1]. These parameters will also affect other components of the resistance. The ratio of spray resistance to total resistance is calculated to evaluate the contribution of spray resistance. The analysis shows that beam has the largest impact on this ratio, and increasing the beam is the most efficient way to increase the spray resistance contribution [1]. Thus, the hull is expected to be designed as wide as possible.

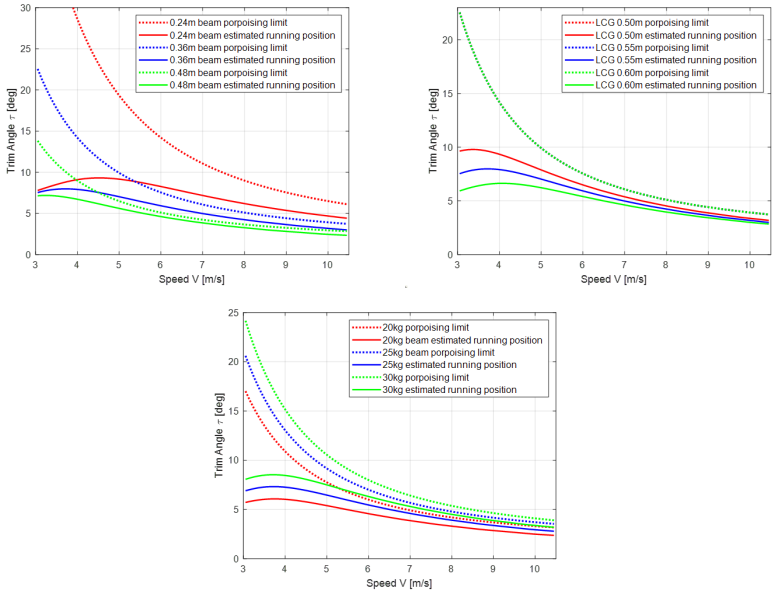

Figure 1. The effect changing one hull parameters on the porpoising limit and running position. Left: Both porpoising limit [1] and running trim angle (Savitsky prediction [1]) increase as beam reduces, but the growth of porpoising limit is notably higher than running trim. Middle: Adjusting position of LCG only affects running trim angle. The more forward the LCG, the lower the running trim angle. Right: With a heavier hull, the porpoising limit [1] and estimated running trim (Savitsky prediction [1]) will increase by a similar amplitude.

Another paramount design consideration is porpoising, which is a common phenomenon for HSC. Porpoising is defined as a coupled motion of heave and pitch due to dynamic instability and causes the hull to jump out of the water periodically[16]. It should be averted in any kind of model experiment, since porpoising may damage the model and invalidate the experimental results due to missing data [17]. To predict the inception of porpoising, empirical formulas given by Savitsky [1] and Celano [17] can be used. These two empirical formulas have different application ranges, and with a low load coefficient C_Δ of 0.34 [16], the Savitsky equation 1 should be used [1] [17].

$$\tau_{crit} = -1.87 + 0.54\sqrt{\frac{C_L}{2}} + 80.87\frac{C_L}{2} + 0.193\beta - 0.0017\beta^2 - 0.312\beta\sqrt{\frac{C_L}{2}} \tag{1}$$

According to equation 1, the porpoising limit and actual running position are affected by three parameters (beam, Longitudinal Center of Gravity (LCG), and weight of hull). To investigate the effects on porpoising by each variable, one parameter is varied at a time, and the result is shown in Figure 1. The dashed line is the porpoising limit 1 and the solid line is the running trim angle predicted by Savitsky [1]. The zone below the dashed line is the stable planing regime and the region above the line indicates a high porpoising probability.

Making the hull more narrow is an effective way to reduce the possibility of porpoising in the design stage. Adding weight to adjust the position of the LCG can be an alternative solution to prevent porpoising, this is easily done during experiments. Although the effect of weight change on porpoising limit is negligible, it is still a good measure to improve the running position.

In the design process, dimensional parameters interact with each other, so compromises have to be made. A hull with a low L/B ratio has a higher contribution of spray resistance, but considering the porpoising risk, the L/B ratio cannot be too low [18]. The deadrise of HSC is usually between 15 and 25 degrees [17]; a higher deadrise angle does not only lower acceleration [19] but increases the spray resistance ratio. However, spray rails function best at deadrise angles below 20 degrees [11].

Model design is an iterative process and many iterations have been carried out to determine the optimal dimensions. The suitable L/B ratio range is 3.5-4 for the design objective and limitations, and it is assumed to be 3.5 in the beginning. ITTC [20] recommends the free running model to be longer than 2m. To allow for future comparisons with towing tank testing, the dimensions of the Davidson Laboratory towing tank were taken into consideration. The length of the model should not exceed half the width of the tank [21], therefore the length should be 2.4m or less. The parameters were inserted into Orca 3D design assistant, and the model was drawn in Rhinoceros. The displacement was calculated in Rhinoceros and used to get the maximum speed needed to reach the desired volumetric Froude number (commonly used as a non-dimension reference value for describing speed in HSC studies [11] [22] [23] because waterline length varies significantly with changing trim angles). The upper limit for the beam can be obtained by empirical formula 1 to predict porpoising with a known weight, speed and trim. If the calculated beam exceeds the allowed beam, raising the L/B ratio or reducing the model length would be necessary to reduce beam. The adjustment is implemented on L/B ratio first since it allows for a large B and thus maintain the same spray resistance contribution. Length starts decreasing if the porpoising limit cannot be satisfied after the L/B ratio exceeds 4. The iteration is repeated until passing the test for potential porpoising. The simplified design iteration flow can be seen in Figure 2. The final model dimensions are listed in Figure 3.

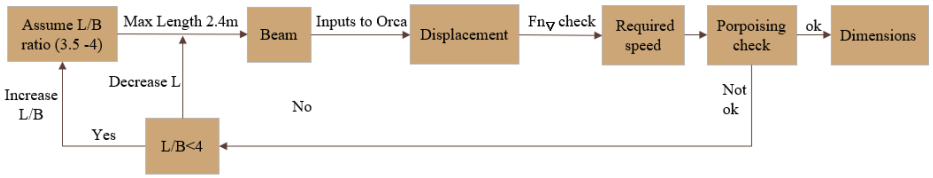

Figure 2. Iteration flow for determining hull parameters

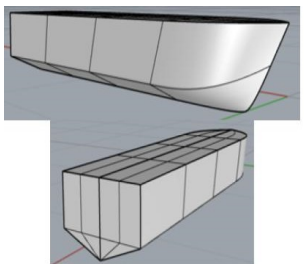

Parameter	Imperial unit	SI unit
Length overall Loa	85 inch	2.16 m
Waterline length Lwl	80 inch	2.02 m
Beam B	21.2 inch	0.54 m
Displacement Δ	47.2 lbs	21.4 kg
Deadrise angle β	20°	20°
LCG	25.6 inch	0.65 m
VCG	6.3 inch	0.16 m

Figure 3. 3D model in Rhino (left) with dimensions (right)

The model is a prismatic hull designed in Orca 3D using parametric definition. Some modifications are implemented to ensure hull continuity and adjust the bow shape. The 3D model in Rhino is shown in Figure 3.

Figure 4 shows the running positions and critical porpoising trim for the model by Molchanov et. al. [2] and the current model. The model by Molchanov et. al. [2] did not experience porpoising, so it is expected that the current model will not porpoise with the similar margin between limit and estimated running trim.

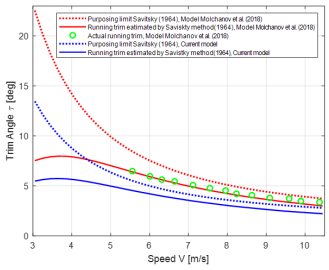

Figure 4. Estimation of the risk of porpoising of the current and the model designed by Molchanov et. al. [2]. The dashed lines are the porpoising limit for models. The blue curves show the running trim estimated by the Savitsky method [1], while the green circles are the running trim measured by Molchanov et. al. [2].

2.2. Propulsion and Power Management System

The propulsion system will provide thrust to the free running model and keep it running at constant speeds. The system includes a brushless DC motor, an ESC (electronic speed control), a drive shaft, and a thruster; however, the final propulsion system has yet to be implemented.

The free running model should be representative of the majority of the HSC in use today, so the Speed to Length Ratio (SLR), equation 2 for the model must be consistent with the SLRs for today's HSC. The vast majority of recreational and utility vessels being produced and used today fall between SLR's of 5 and 10, see Figure 5 (The Length overall (LOA) was used since it is more readily available than the Length at the Waterline (LWL). To obtain a SLR just short of 10, a model with a length of 2.16 m will need to be capable of reaching speeds of up to 25 knots.

$$SLR = \frac{v}{\sqrt{L}}\left[\frac{Knots}{\sqrt{ft}}\right] \tag{2}$$

The resistance was estimated by the Savitsky Method [1] after deciding the running speed. The thrust deduction should be considered to determine the required thrust due to the effect of the thruster [24]. Then the required power for the DC motor can be calculated. The thrust and power at different speeds are shown in Figure 6. The required thrust for the highest running speed is 128N and the required power is about 1KW.

To determine the required powered for the DC motor revolution speed and torque must be chosen according to the dimensions of the thruster. The propeller diameter should be larger than 10 cm for a more accurate measurement of torque [20]. However, for podded vessels, which act like an azimuth thruster, instantaneous modifications will have to take place to achieve a constant torque [20]. Most propellers found on the market

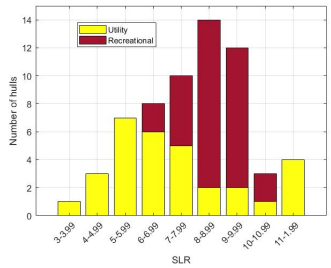

Figure 5. Maximum SLR for 31 utility vessels (yellow) and 31 recreational vessels (red).

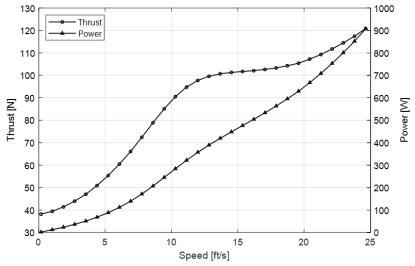

Figure 6. Thrust and power estimated by Savitsky method [1]

with a 10 cm diameter have a pitch to diameter ratio (P/D) of about 1.0. For this P/D ratio, the propeller chart by Molland et al. [24] gives the thrust coefficient K_T as 0.22 and the torque coefficient K_Q as 0.036. The selected thruster is shown in Table 1.

Table 1. Costs and specifications for powering components

Thruster	**Cost Per Unit (USD)**	**Thrust (N)**	**Weight (kg)**	**Location**
Lewmar Gen2 Bow Thruster	1,826.44	637.432	20	Hodgesmarine.com
DC Motor	**Cost Per Unit (USD)**	**Power (kW)**	**Max RPM**	**Location**
Turnigy AquaStar	112.91	5.28	21900	hobbyking.com
Speed Controller Sensor	**Cost Per Unit (USD)**	**Component**	**Weight (kg)**	**Location**
Infrared Sensor	11	OSOYOO LYSBO1157HIJO	0.045	Amazon.com
Battery	**Cost Per Unit (USD)**	**Capacity (mAh)**	**Volts (V)**	**Location**
URUAV 5S	88.48	6200	18.5	alexnld.com

The advancing speed of the model depends on the RPM of the motor and the diameter of the thruster, and the RPM should be larger than 4600 according to equation 3. The thrust coefficient (equation 4) is used to check if the thruster can provide enough thrust at this RPM [24]. At a thrust of 129N at 4600RPM, it exceeds the maximum thrust needed. The motor is chosen with a a minimum RPM capability of approximately 5000, to provide a safety margin. The torque requirement of 2.2Nm was determined using equation 5. [24].

$$RPM > V_{max}/pitch \tag{3}$$

$$T = \rho n^2 D^4 K_T \tag{4}$$

$$Q = \rho n^2 D^5 K_Q \tag{5}$$

A speed controller is required to keep the model running at a constant speed. The running speed and motor speed are different reference parameters, so controlling the running speed directly through motor speed is not a fast or efficient way. To isolate the problem, the speed control system has a cascaded structure. There are two loops in the entire control process. The inner loop is for motor speed control. The motor can be modelled in Simulink, see Figure 7. The outer loop is a direct adjustment to the speed. The running position varies at different speeds, so it is hard to find a transfer function to

relate the motor speed to the running speed. The free running model will run at different speeds first, and the motor speed input and running speed output will be used to find transfer functions by system identification.

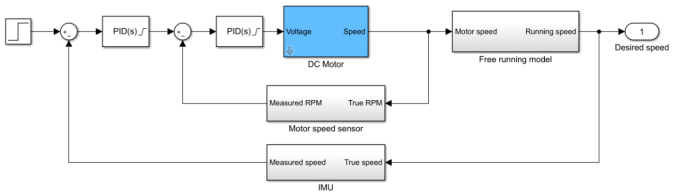

Figure 7. Speed control flow chart

An infrared sensor is needed to measure the RPM of the DC motor. Since the resistance measurement is difficult for the free running model, shaft thrust is measured by a dynamometer to assess the dynamic performance. The higher the shaft thrust, the closer the model is to reaching the self-propulsion point where the thrust equals the resistance with added propellers [25]. The difference between this resistance and the resistance of the model without added propellers is the thrust deduction [25]. A list of electronics and sensors needed for the speed controller are shown in Table 1.

To power the DC motors, batteries will need to be charged and inserted in the hull before testing. Being able to remove the batteries from the hull will be crucial so that we can have multiple pre-charged replacement batteries on hand for testing. This will significantly increase the testing time. We will use multiple lithium polymer (LiPo) batteries, similar to ones that have been used in other free running models [7]. Based on Larson's design [7], we will use multiple batteries that can be connected in parallel, to allow for battery replacement, and then those sets of batteries will be connected in series. The sets of batteries that are connected in parallel will be charged and replaced as a single unit. Possible batteries that can be used in the model are shown in Table 1 with their prices and specifications.

2.3. Steering

Three control systems (proportional-integral-derivative (PID) controllers, fuzzy logic controllers, and backstepping controllers [26] [27]) have been examined with respect to the effectiveness, the complexity of constructing each model, and previous controllers chosen for free running model tests. A gain scheduling PID controller was chosen for our free running model because it has a simple input-output case, and has a long history of conventional control [26] that is less complex than fuzzy-logic controllers[28] and backstepping controllers [29]. The typical control law u(t) of a PID controller is given by,

$$u(t)=K_p e(t)+K_i \int e(t)d\tau+K_d \frac{d}{dt} e(t) \tag{6}$$

where e(t) defines the error signal, Kp defines the proportional gain, Ki defines the integral gain, and Kd defines the derivative gain [26]. The desired trajectory has the model run in a straight line. To accomplish this, we have designed a guidance and PID controller in MATLAB and Simulink. The control system is composed of the controller, Global

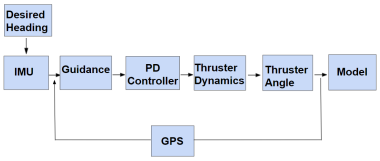

Figure 8. Control System Block Diagram

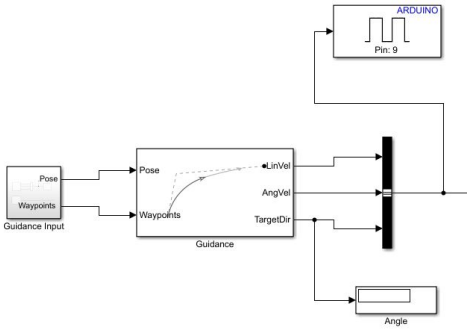

Figure 9. Simulink Model of Guidance System

Positioning System (GPS) and an Inertial Measurement Unit (IMU) which will be connected to an Arduino board. For the purpose of our free running model, a thruster will be used instead of a rudder; thrusters provide a duel-purpose for the model in acting as part of the propulsion and steering system, whereas rudders only aid with steering the vessel and can be more easily damaged. The block diagram of the control system is shown in Figure 8.

The system depends on the collected IMU data from the Arduino to determine the current position of the free running model. The PID controller takes the error of the system between the input and output and makes corrections to the thruster to reach the desired angle [30]. The input of the system is the model's current position, taken from the GPS and IMU. The free running model's desired heading is expected to be zero degrees. To ensure that the model follows the desired heading, it will follow a series of waypoints [31]. Waypoints are a set of predetermined targets the model must hit to follow the planned path towards a lookahead distance. As the model gets closer to a given waypoint, the heading error is reduced and the planned trajectory can be more accurately tracked [31]. The Simulink model of the guidance system is shown in Figure 9.

The output of the system is the thruster angle. The transfer function of the feedback system relating the current heading angle with the outputted thruster angle is given by, $h(s) = \frac{0.847}{s^2+1.55s+0.918}$ [32]. The gains were tuned using the PID tuner tool in MATLAB. Adjusting the K_i gain resulted in an unstable system, so a PD controller was chosen. The parameters decided came to be $K_p = 78.5$ and $K_d = 17$. These parameters may be adjusted when we run simulations to test the controller. The thruster dynamics block of the controller allows the system to communicate with the sensors and brushless DC motor to actuate the thruster to steer in the desired trajectory.

To test the controller, an Adafruit BNO055 orientation sensor, a HC-SR04 ultrasonic sensor, and a TOYEN remote control high speed racing boat were wired to an Arduino Uno board. The purpose of the toy boat is to only test the control system, consisting of the guidance system and PD controller, to ensure the model runs in a straight path as desired. The display of the set-up is shown in Figure 10. The testing that took place in a swimming pool can be seen in Figure 11. Our model will consist of a thruster; however, the remote control boat utilizes a rudder, which should not affect the PD controller.

Full integration of the Simulink model with the remote control boat equipped with an Arduino board is still under development. Adjustments to the controller will be made

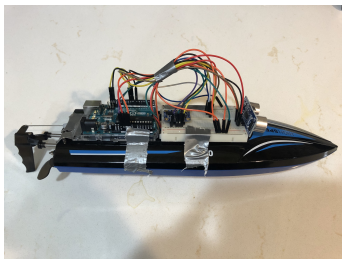

Figure 10. Remote Control Boat Wiring Set-Up

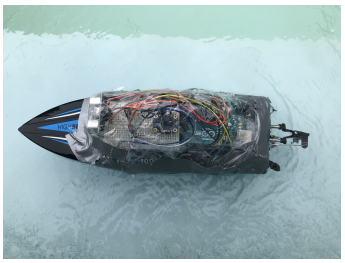

Figure 11. Remote Control Boat Pool Test

according to the results of the test runs. Further testing is necessary to improve the PD controller to make a proper connection with the Arduino board.

2.4. Sensors

An Arduino microcontroller will be used to process all sensor data and control the navigation and guidance system with the PD controller. The guidance, navigation, and control system will consist of an inertial measurement unit (IMU), Global Positioning System (GPS), digital compass, and remote control receiver [29]. A GPS will communicate with the model to determine its current location on the water. An IMU consists of an accelerometer, gyroscope, and magnetometer to measure velocity, orientation, and gravitational forces of the free running model during operation [29]. The digital compass contributes to the heading and orientation of the model. The remote control receiver is necessary to pair with a transmitter in the event where manual control of the model needs to be taken over. A LIDAR sensor for ranging to keep track of the planned trajectory will also be included. A WiFi router will be used to telemeter the data from the free running model to the ground station computer. The running trim will be recorded by an inclinometer. The estimated costs of potential sensors are listed in Table 2.

Table 2. Sensor Costs

Item	Component	Cost Per Unit (USD)	Weight (kg)	Location
GPS	Spot Trace GPS	100	0.088	Rei.com
IMU	XSENS MTI-7-T	406	0.016	Mouser.com
Digital Compass	PNI RM3100 Magnetometer	36	0.017	Amazon.com
RC Reciever	FrSky 8XR	36	0.017	Amazon.com
RC Transmitter	FrSky Taranis X9D	218	0.67	Amazon.com
LIDAR Sensor	LIDAR-Lite 3 Laser Rangefinder	130	0.016	Robotshop.com
WIFI Router	ASUS RTN66U 5GHZ Router	304	0.816	Amazon.com

3. Environment Monitoring and testing site

Fridsma [33] performed wave tests at significant wave height to hull beam ratio ($H_{1/3}$/B) of 0.222, 0.444 and 0.666. Nevertheless, these sea states could be too severe for small HSC [34]. Moreover, unlike the towing tank test, the free running has six degrees of

freedom, so the response to the wave would be more aggressive. In recent HSC model experiments $H_{1/3}$/B from 0.15 to 0.25 are commonly used [35] [36] [37] [38]. Therefore, $H_{1/3}$/B = 0.2 is chosen, leading to a significant wave height of $H_{1/3}$ = 0.108m. Observed wave heights often follow the Rayleigh distribution, and relationship between peak period Tp and $H_{1/3}$ can be calculated based on this distribution and the peak period Tp = 1.64s when $H_{1/3}$ = 0.108m.

To maintain a log of the conditions accompanying each run we will deploy two wave buoys at the testing site to account for changes in the seabed or wind. The wave buoys should be small enough to deploy and remove from the water for each testing session. It would be ideal for the wave buoy to be capable of monitoring more than the wave conditions, such as water temperature and water current strength, as fewer accompanying instruments will be required. In Table 3, several options for wave buoys and their characteristics are listed for comparison. To supplement the monitoring of wave characteristics we will use an ultrasonic sensor similar to the one mounted on the carriage of the Davidson Laboratory High Speed Towing Tank. The sensor could possibly be mounted to the front of the free running model, as long as the added weight of the sensor does not significantly alter the behavior of the hull. A list of possible ultrasonic sensors and their costs are shown above in Table 3, the brand that is used in the Davidson Laboratory is first on the list of ultrasonic sensors.

Table 3. Wave Buoys and Ultrasonic Sensors

Name	Cost Per Unit (USD)	Diameter (cm)	Weight (kg)	Location
Wave Buoys				
Spotter V2	4900	42	5.4	sofarocean.com
Wavesense	NA	Placed on Buoy	Placed on Buoy	fugro.com
Micro Wave Buoy	NA	50	33.5	hiseamarine.com
TRIAXYS Mini Wave Buoy	32000	60	60	axystechnologies.com
Mini Wave Buoy	NA	60	$\leq$50	hiseamarine.com
Ultrasonic Sensors				
ToughSonic 3	NA	33.4	0.4	senix.com
BUS0039	277.09	30	NA	balluff.com
UK1F-E4-0A	158	18	NA	automationdirect.com
Banner Engineering	252.73	18	NA	alliedelec.com
Pepperl+Fuchs	415.15	30	0.1406	wolfautomation.com

Our tests will be carried out in a site near Texas A&M University Galveston Campus. Here the sea states range from very calm to fairly rough depending on the conditions. Finding water that is clear enough to take underwater photos of our model during runs would require testing 10-20 nautical miles offshore, which would not be ideal for convenience of adjustments and repairs throughout testing.

4. Conclusions

The design of a model scale HSC for free running tests has be developed. The hull has been designed with focus on evaluation of spray deflection technologies while avoiding porpoising [18]. The model length of just over 2 m, is consistent with the size of previous

free running models [39] [8] [10]. The propulsion system (comprised of a DC motor, electronic speed control, drive shaft, and thruster) will be capable of replicating speeds that are consistent with the majority of HSC used today. A Simulink model for an autonomous course keeping system that uses a PD controller with an IMU was developed. Preliminary implementation of the steering system with a remote control hobby boat was carried out, but more work still needs to be done to successfully integrate the systems. Methods for monitoring the outdoor environment using floating wave buoys and/or ultrasonic sensors mounted to the model were explored and specific instrument options were presented. The requirements and desired characteristics of a future testing site are outlined and a testing location has been found off the coast of Texas A&M University Galveston Campus. This paper has found a very pressing need for free running tests for HSC in hydrodynamics research, and has made a detailed proposal for such testing that will be carried out in the near future.

5. Acknowledgements

This work was sponsored by the Office of Naval Research, ONR award number N00014-20-1-2490, Robert Brizzolara is the program manager and Stevens Institute of Technology Innovation & Entrepreneurship Undergraduate Summer Research Program, Mary Ann Piazza is the program lead. We would also like to thank Jonas Danielsson, Petestep AB and Bogdan Molchanov for their useful feedback and advice.

References

[1] Savitsky, D. (1964) *Hydrodynamic design of planing hulls*. Marine Technology, 1:71–95.

[2] Molchanov, B., Lundmark S., Fürth M., Green M. (2019) *Experimental validation of spray deflectors for high speed craft*. Ocean Engineering, 1:71–95.

[3] Seo, J., Choi, H., Jeong, U., Lee, D.K., Rhee, S.H., Jung, C.M., Yoo, J. (2016) *Model tests on resistance and seakeeping performance of wave-piercing high-speed vessel with spray rails*. International Journal of Naval Architecture and Ocean Engineering.

[4] Lakatos, M., Sahk, T., Kaarma, R., Tabri, K. and Kõrgesaar, M. (2019) *Experimental testing of spray rails for the resistance reduction of planing crafts*. 7th International Conference on Marine Structures.

[5] Judge, C., Mousaviraad, M., Stern, F., Leed, E., Fullertond, A., Geiser, G., Schleicher, C., Merrill, C., Weil, C., Morin, J., Jiang, M., Ikeda, C. (2020) *Experiments and CFD of a high-speed deep-V planing hull—Part I: Calm water*. Applied Ocean Research, 96, 102060.

[6] Jiao, J., Sun, S., Li, J., Adenya, A. C., Ren, H. Chen, C., and Wang, D. (2018) *A comprehensive study on the seakeeping performance of high speed hybrid ships by 2.5D theoretical calculation and different scaled model experiments*. Ocean Engineering 160, 197–223.

[7] Larson, S. (2015) *Design and Construction of Unmanned Surface Vehicles*. Lehigh University.

[8] Kim, D. J., Kim, S. Y. (2017) *Turning characteristics of waterjet propelled planing boat at semi-planing speeds*. Ocean Engineering, 143, 24–33.

[9] Lewandowski, E. (1995) *Free Running Model Turning Tests of the U.S. Coast Guard 47 FT Motor Life Boat*. U.S. Coast Guard Research and Development Center.

[10] Benjamin Friedhoff, F., Feller, U. (2014) *Free Running Model Tests of High Speed Craft to Complement Tank Testing*. Conference: 4th International Conference on Advanced Model Measurement Technologies for the Maritime Industry.

[11] Clement, E.P. (1964) *Effects of longitudinal bottom spray strips on planing boat resistance*. Navy Dept., David Taylor Model Basin.

[12] Olin, L. (2017) *Numerical modelling of spray sheet deflection on planing hulls*. Proceedings of the Institution of Mechanical Engineers.

[13] Wielgosz, C., Fürth, M., Datla, R., Chung., U., Rosén, A., Danielsson, J. (2018) *Experimental validation of numerical drag prediction of novel spray deflector design*. 13th International Marine Design Conference.

[14] Savitsky, D., DeLorme, M., Datla, R. (2007). *Inclusion of Whisker Spray Drag in Performance Prediction Method for High-Speed Planing Hulls*. Marine Technology, 44, 35-56.

[15] Larsson, L. and Raven, H. C. (2010). *Principles of Naval Architecture Series: Ship Resistance & Flow*. Society of Naval Architects and Marine Engineers (SNAME).

[16] Day, J.P. and Haag, R.J. (1952) *Planing Boat Porpoising*. ebb Institute of Naval Architecture.

[17] Celano, T. (1998) *The prediction of porpoising inception for modern planing craft*. U.S. Naval Academy.

[18] Masumi, Y. and Nikseresht, A.H. (2017) *Comparison of numerical solution and semi-empirical formulas to predict the effects of important design parameters on porpoising region of a planing vessel*. Applied Ocean Research.

[19] Larsson, L., Eliasson, R. (2000) *Principles of yacht design*. International Marine.

[20] ITTC (2014) *Free Running Model Tests*. 27th International Towing Tank Conference, Recommended Procedures and Guidelines, Procedure 7.5-02-01-01.

[21] ITTC (2014) *Captive model test procedures*. 27th International Towing Tank Conference, Recommended Procedures and Guidelines, Procedure 7.5-02-06-02.

[22] Savitsky, D. (1985) *Planing Craft*. Naval Engineers Journal, 97, 113-141.

[23] Almeter, J. (1993) *Resistance prediction of planing hulls: State of the art*. Marine Technology.

[24] Molland, A., Turnock, S., Hudson, D. (2017) *Wake and Thrust Deduction. In Ship Resistance and Propulsion: Practical Estimation of Ship Propulsive Power (pp. 149-173)*. Cambridge University.

[25] Tupper, C. (2013) *Chapter 8 - Propulsion*. Introduction to Naval Architecture, 5, 161 - 203.

[26] Menoyo Larrazzabal, J., Santos Peñas, M. (2016) *Intelligent Rudder Control of an Unmanned Surface Vessel*. Expert Systems with Applications, 55, 106 -117.

[27] Sonnenburg, C. R., Woolsey, C. A. (2013) *Modeling, Identification, and Control of an Unmanned Surface Vehicle*. Journal of Field Robotics, 30(3), 371-398.

[28] Hossain, Md. F. (2019) *Chapter 7: Public Transportation Systems*. Sustainable Development for Mass Urbanization, Elsevier, 77-109.

[29] Sarda, E.I., Qu, H., Bertaska, I.R., von Ellenreider, K.D. (2016) *Station-Keeping Control of an Unmanned Surface Vehicle Exposed to Current and Wind Disturbances*. Ocean Engineering, 127, 305 - 324.

[30] Demetriou, G.A., Ioannnou, S., Hajipieris, A., Panayidou, I., Papasavva, A. (2016) *ERON: A PID Controlled Autonomous Surface Vessel*. 18th Mediterranean Electrotechnical Conference.

[31] Li, C., Jiang, J., Duan, F., Lui, W., Wang, X., Bu, L., Sun, Z., Yang, G. (2019) *Modeling and Experimental Testing of an Unmanned Surface Vehicle with Rudderless Double Thrusters*. Sensors.

[32] Fan, Y., Mu, D., Zhang, X., Wang, G., Guo, C. (2018) *Course keeping Control Based on Integrated Nonlinear Feedback for a USV with Pod-like Propulsion*. Journal of Navigation, 71(4), 878-898.

[33] Fridsma, G. (1971) *A systematic study of the rough-water performance of planing boats: (irregular waves - part II)*. Davidson Laboratory, Stevens Institute of Technology.

[34] Rosén, A., Begovic, E., Razola, M. and Garme, K. (2017) *High-speed craft dynamics in waves: challenges and opportunities related to the current safety philosophy*. 16th International Ship Stability Workshop.

[35] Begovic, E., Bertorello, C., Pennino, S. (2014) *Planing Hull Seakeeping In Irregular Head Seas*. Transactions of Famena, 38, 1-12.

[36] Katayama, T., Amano, R. (2016). *An Experimental Study on the Characteristics of Vertical Acceleration on Small High Speed Craft in Head Waves*. Journal of the Japan Society of Naval Architects and Ocean Engineers 23:65-76.

[37] Begovic, E., Bertorello, C., Pennino, S., Piscopo, V., Scamardella, A. (2016). *Statistical analysis of planing hull motions and accelerations in irregular head sea*. Ocean Engineering, 112, 253-264.

[38] De Luca, F., Pensa, C. (2019). *The Naples Systematic Series – Second part: Irregular waves, seakeeping in head sea*. Ocean Engineering, 194, 106620.

[39] Kim, J., Wang, Y., and Nguyen H. (2017) *Modelling and Simulation of a Surface Vessel by Experimental Approach with Low-Cost Sensors* . 11th Asian Control Conference.